Influence of Multiple Metal Ions on β-Amyloid Aggregation and Dissociation on a Solid Surface†

Jungki Ryu,‡ Koyeli Girigoswami,‡ Chanki Ha,§ Sook Hee Ku,‡ and Chan Beum Park*,‡,§

Institute for the BioCentury and Department of Materials Science and Engineering, Korea Advanced Institute of Science and Technology, 373-1 Guseong-dong, Yuseong-gu, Daejeon, Republic of Korea, and Science and Engineering of Materials Interdisciplinary Program, Arizona State University, Tempe, Arizona 85287

Received January 4, 2008; Revised Manuscript Received March 20, 2008

ABSTRACT: Recently discovered evidences suggest that precipitation of Alzheimer's β-amyloid (Aβ) peptide and the toxicity in Alzheimer's disease (AD) are caused by abnormal interactions with neocortical metal ions, especially Zn^{2+}, Cu^{2+}, and Fe^{3+}. While many studies had focused on the role of a "single" metal ion and its interaction with Aβ peptides, such studies involving "multiple" metal ions have hardly been explored. Here, to explore the nature of codeposition of different metals, two or more metal ions along with Aβ were incubated over a solid template prepared by immobilizing Aβ42 oligomers. The influence of Zn^{2+}, Cu^{2+}, and Fe^{3+} on Aβ aggregation was investigated by two approaches: co-incubation and sequential addition. Our results using ex situ AFM, ThT-induced fluorescence, and FTIR spectroscopy indicated that the co-incubation of Cu^{2+}, Zn^{2+}, and Fe^{3+} significantly altered the morphology of aggregates. A concentration dependence study with mixed metal ions suggested that Zn^{2+} was required at much lower concentrations than Cu^{2+} to yield nonfibrillar amorphous Aβ deposits. In addition, sequential addition of Zn^{2+} or Cu^{2+} on fibrillar aggregates formed by Fe^{3+} demonstrated that Zn^{2+} and Cu^{2+} could possibly change the conformation of the aggregates induced by Fe^{3+}. Our findings elucidate the coexistence of multiple metal ions through their interactions with Aβ peptides or its aggregates.

Alzheimer's disease (AD)[1] is a progressive neurodegenerative disorder associated with the pathological self-assembly of β-amyloid (Aβ) peptide into toxic soluble oligomers and insoluble fibrils with high cross β-sheet content (*1*). The amyloid deposits in the brains of individuals with AD originate from a proteolytic byproduct of the transmembrane β-amyloid precursor protein (APP) (*2, 3*). However, researchers have yet to reach a consensus with regard to either the nature of Aβ processing or its aggregation. Investigators have found that the different forms of Aβ aggregates exerted different extents of toxicity in cells. Aβ oligomers were reported to inhibit neuronal viability 10-fold more than fibrils in Neuro-2A neuroblastoma cells (*4*−*6*). On the other hand, some studies explicated that fibrillar Aβ aggregates, but not the amorphous aggregates of Aβ, cause neuronal cell death (*7*−*9*). Thus, according to the literature, the degree and the nature of aggregation of Aβ peptide decide the extent of neurotoxicity, suggesting that Aβ aggregation is certainly an essential event in the pathogenesis of AD.

Metal ions had been proposed to play a significant role in the assembly and neurotoxicity of AD fibrils (*10*), although the mechanism leading to the conformational change of soluble Aβ peptides into insoluble amyloid plaque is unclear (*11*). Transition metals such as copper (Cu), iron (Fe), and zinc (Zn) were also identified at high concentrations in the Aβ plaques (∼400 μM Cu, ∼1 mM Zn, and ∼1 mM Fe) (*10, 12*) and contributed to the neuropathology associated with Aβ fibrils by affecting the rate of fibril formation (*13*−*15*), by modifying fibril morphology (*16, 17*), and by direct chemical reaction with Aβ (*18, 19*). Although the findings of several studies have highlighted the role of a "single" metal ion and its interaction with Aβ peptide and aggregation (*20*−*22*), such studies involving "multiple" metal ions together with Aβ have hardly been explored. As in the brains of AD patients the different metals coexist at higher than normal concentrations, further study of the effects of multiple metal ions interacting with Aβ is warranted. In this work, we sought to explore the various natures and extents of Aβ aggregates formed in the presence of multiple metal ions, such as Cu^{2+}, Zn^{2+}, and Fe^{3+}.

While previous studies involving the effect of metal ions on Aβ-associated aggregation measured the overall level of aggregation in a "solution" phase (*13, 23, 24*), here we used a "solid" template system that was prepared by the chemical immobilization of Aβ oligomers as a seed onto a NHS-activated solid surface. The fibrillar growth of Aβ over the

† This study was supported by grants from the Korea Research Foundation (KRF-2006-D00078) and the National Institute of Health (1R21AG024114−01A2).

* To whom correspondence should be addressed. Phone: +82-42-869-3340. Fax: +82-42-869-3310. E-mail: parkcb@kaist.ac.kr.

‡ Korea Advanced Institute of Science and Technology.

§ Arizona State University.

[1] Abbreviations: Aβ, β-amyloid; AD, Alzheimer's disease; AFM, atomic force microscopy; FTIR, Fourier transform infrared; ThT, thioflavin T; PSD, power spectral density; HFIP, 1,1,1,3,3,3-hexafluoro-2-propanol; Me_2SO, dimethyl sulfoxide; APTS, 3-(aminopropyl)triethoxysilane; DSC, *N*,*N*′-disuccinimidyl carbonate; NHS, *N*-hydroxysuccinimide ester; BSA, bovine serum albumin; HSA, human serum albumin; MTT, 3-(4,5-dimethylthiazol-2-yl)-2,5-diphenyltetrazolium bromide.

10.1021/bi800012e CCC: $40.75
Published on Web 04/19/2008

solid template was plaquelike as confirmed in our previous studies by ex situ atomic force microscopy (AFM), thioflavin T (ThT)-induced fluorescence, and Fourier transform infrared (FTIR) spectroscopy (*25, 26*). To use Cu^{2+}, Zn^{2+}, and Fe^{3+} conjointly for the study of Aβ aggregation and deposition due to the competition between the multiple metal ions, our investigation was grouped into two different sets of experiments: (1) co-incubation and (2) sequential addition. In the co-incubation experiments, two or three metal ions were incubated together with fresh Aβ monomers dissolved in a buffer solution over the oligomer-seeded, solid template surface. In contrast, the sequential addition experiments were conducted for the preformed, Fe^{3+}-induced Aβ aggregates. The template containing Fe^{3+}-induced, fibrillar deposits of Aβ was further incubated in a solution containing either Zn^{2+} or Cu^{2+}. In both sets of experiments, the templates were washed and dried, followed by the observation of the surface using multiple analytical tools. The morphology of the Aβ deposits over the templates was analyzed by ex situ AFM, whereas FTIR spectroscopy and ThT-induced fluorescence analysis revealed the chemical differences of those aggregates. According to our results, Cu^{2+} and/or Zn^{2+}, when co-incubated with Fe^{3+}, prevented Aβ from participating in fibril formation, resulting in the formation of amorphous, nonfibrillar aggregates. Upon the sequential addition of Zn^{2+} and/or Cu^{2+} to preformed fibrillar aggregates induced by Fe^{3+}, there was a significant decrease in the amount of fibrillar deposits, yielding amorphous aggregates. The results highlighting the effect of Zn^{2+} and Cu^{2+} on pre-existing fibrillar aggregates are highly significant as they provide clear evidence that the proper concentrations of different metal ions may even decrease the extent of Aβ fibrillation. This study elucidates the coexistence of multiple metal ions through their interactions with Alzheimer's Aβ peptides or their aggregates.

MATERIALS AND METHODS

Materials. Human β-amyloid (Aβ) 42 was obtained from rPeptide Co. (Athens, GA). Bovine serum albumin (BSA), human serum albumin (HSA), 3-(aminopropyl)triethoxysilane (APTS), *N*,*N*′-disuccinimidyl carbonate (DSC), 1,1,1,3,3,3-hexafluoro-2-propanol (HFIP), dimethyl sulfoxide (Me_2SO), thioflavin T (ThT), $CuCl_2 \cdot 2H_2O$, $ZnCl_2$, $FeCl_3$, histidine, glycine, sodium citrate, and 3-(4,5-dimethylthiazol-2-yl)-2,5-diphenyltetrazolium bromide (MTT) were purchased from Sigma-Aldrich (St. Louis, MO). Culture media and supplements were obtained from Welgene Co (Korea). Microcover glasses were obtained from VWR Scientific (West Chester, PA). Pre-existing Aβ peptide aggregates were disintegrated into fresh monomers as described previously (*25*). Briefly, the peptides were dissolved in HFIP, sonicated in a water bath, and then aliquoted into sterile Eppendorf tubes. After the complete vaporization of HFIP, an Aβ peptide film was formed on the wall of the tubes which was then stored at −20 °C. Immediately prior to use, the Aβ peptide film was dissolved in Me_2SO and then diluted with phosphate-buffered saline (PBS, pH 7.4) or 20 mM Tris buffer (TB, pH 7.4 at 37 °C) to a desired concentration. The final concentration of Me_2SO in the peptide solution was kept at 5% (v/v).

Preparation of Solid Aβ Template. Aβ templates were prepared by covalently immobilizing oligomeric Aβ seeds onto microcover glass as described previously (*25*). Briefly, cover glasses were cleaned with a piranha solution (70% H_2SO_4/30% H_2O_2), rinsed extensively with distilled water, and dried. A hydroxyl-terminated glass surface was then reacted with 3% APTS in 95% ethanol and further cured at 110 °C with 100% ethanol. For the activation of these glass surfaces with NHS, they were incubated in 20 mM DSC in sodium bicarbonate buffer (50 mM, pH 8.5). The slides were washed with deionized water and dried with N_2. An oligomeric Aβ solution, prepared by preincubating a 30 μM fresh Aβ solution in PBS at 37 °C for 12 h, was then uniformly placed onto a NHS-activated glass surface. Remaining unbound NHS-activated sites were then blocked with a 0.1% solution of BSA in 50 mM phosphate buffer (PB, pH 7.5). Noncovalently adsorbed oligomers were removed from the glass slides when they were extensively washed with 50 mM PB (pH 7.5) and deionized water and were then dried with N_2.

Co-Incubation of Aβ Templates in the Presence of Metal Ions. Aβ templates were further incubated in a freshly prepared 6 μM Aβ solution in 20 mM TB (pH 7.4 at 37 °C) containing 5% Me_2SO (v/v). To evaluate the effect of single or multiple metal ions on the deposition of Aβ on a solid surface, the templates were incubated in a Aβ solution with the different concentrations of metal ions (10, 50, and 100 μM), which were controlled by dissolving an appropriate amount of metal salts such as $FeCl_3$, $ZnCl_2$, and $CuCl_2$. After being incubated for 24 h at 37 °C, the templates were taken out of the peptide solution, repeatedly washed with a buffer solution and deionized water, and then dried with N_2 for further analysis. The insoluble hydroxides formed during the incubation with $CuCl_2$, $ZnCl_2$, or $FeCl_3$ may affect the Aβ aggregation morphology, so we checked the binding of small low-affinity ligands for these metal ions. Glycine, histidine, and sodium citrate, the ligands for Cu^{2+}, Zn^{2+}, and Fe^{3+}, respectively, were used in a stoichiometric metal:ligand ratio of 1:6 as described by Huang et al. (*27*). According to our observation, there was a negligible effect on the morphology of Aβ deposits formed over the template in the presence of these ligands compared to those without any ligand (data not shown). Thus, further experiments were carried out in the absence of such ligands. With regard to the effect of NaCl on metal-induced Aβ aggregation, it was seen in our previous work with single metal ions (*26*) that there was a negligible effect of NaCl concentration on Cu^{2+}-, Zn^{2+}-, and Fe^{3+}-induced Aβ aggregation on a solid surface. Therefore, here we did not extend our experiments involving multiple metal ions in the presence of NaCl.

Sequential Addition of Zn^{2+} or Cu^{2+} on an Fe^{3+}-Induced Fibrillar Aβ Template. Fe^{3+}-induced fibrillar Aβ templates were prepared by incubating oligomer-immobilized solid templates in a 6 μM Aβ solution in 20 mM TB (pH 7.4 at 37 °C) containing both 5% Me_2SO and 100 μM Fe^{3+}. After being incubated for 24 h at 37 °C, templates were extensively washed with deionized water and dried with N_2. Fe^{3+}-induced fibrillar templates were then put into either pure 20 mM TB or 20 mM TB containing 100 μM Cu^{2+} or Zn^{2+} and incubated at 37 °C for an additional 24 h. After being incubated, those templates were washed with 20 mM TB and further with deionized water for 1 h and dried in a stream of N_2.

Atomic Force Microscopy (AFM). Morphological analysis of Aβ deposits formed by interaction between Aβ peptides and metal ions on a solid template (9 mm × 9 mm) was achieved by ex situ AFM, using a Multimode AFM instrument equipped with a Nanoscope IIID controller (Digital Instruments Inc., Santa Barbara, CA), under ambient conditions. AFM analysis was carried out in the tapping mode in air under the following conditions: scan rate, 1−1.5 Hz; an "E" scanner; a NCHR silicon cantilever (Nanosensors Inc., Switzerland); resonant frequency range of AFM cantilevers, 250−350 kHz; number of pixels, 512 × 512. Representative images in each case were obtained by scanning different samples at four randomly selected spots over the entire template. AFM images were further processed with Nanoscope software provided by the manufacturer of the AFM instrument to produce the height−frequency distribution and power spectral density (PSD). The PSD plot was obtained by the fast Fourier transformation (FFT) operation of wave function for surface features over the entire surface and directions, which provided useful information about surface features in terms of spatial frequency (*28*).

Thioflavin T-Induced Fluorescence. The formation of Aβ aggregates on a solid template was quantitatively assayed by measuring ThT-induced fluorescence using a Victor3 microplate reader (PerkinElmer Inc., Waltham, MA). Samples (9 mm × 9 mm) were prepared as described above, cleaned with deionized water, and dried in a stream of N_2. Each of the solid templates was placed into individual wells of a 24-well plate (SPL Life Sciences, Korea) and then filled with 1 mL per well of a 50 μM ThT solution in TB (20 mM, pH 8.0). Experiments were carried out in triplicate with excitation and emission at 450 and 485 nm, respectively, taking the fluorescence of a bare cover glass as a reference. The average and standard deviation were calculated for data analysis.

Fourier Transform Infrared (FTIR) Spectroscopy. Samples were prepared for FTIR analysis by incubating a solid template (4.5 mm × 7 mm) in a solution containing a freshly prepared 6 μM Aβ42 solution in the absence or presence of 100 μM Fe^{3+} only, 100 μM Fe^{3+} and 100 μM Cu^{2+}, 100 μM Fe^{3+} and 100 μM Zn^{2+}, or 100 μM Fe^{3+}, 100 μM Cu^{2+}, and 100 μM Zn^{2+} incubated in a 20 mM TB solution containing 5% Me_2SO (v/v) (pH 7.4 at 37 °C) for 24 h. After incubation, the samples were cleaned and dried before FTIR measurements were taken. Solid samples were directly placed on a rounded diamond crystal. IR measurements of the solid samples were preformed on a Nicolet Nexus 470 spectrometer (Thermo Nicolet Corp., Madison, WI) equipped with an attenuated total reflection (ATR) accessory. The absorbance spectra of different Aβ samples were collected at a resolution of 4.0 cm^{-1} by subtracting the background spectrum of a plain glass from the sample spectra.

RESULTS

Co-Incubation of Multiple Metal Ions. To study the effect of multiple metal ions on Aβ aggregation over a solid template, the surfaces prepared by immobilizing fresh monomeric or oligomeric Aβ were incubated with a fresh Aβ solution in the presence of one, two, or three different metal ions, namely, Cu^{2+}, Zn^{2+}, and Fe^{3+}. The AFM analysis of the samples of Aβ preincubated for 12 h that were immobilized as a seed indicated the presence of oligomeric species, as shown in our previous study (*25*). The template-induced Aβ aggregation in the presence of multiple metal ions was further characterized through ex situ AFM analysis after incubation for 24 h. Figure S1 of the Supporting Information depicts the aggregation of Aβ over the solid surface at 0 and 24 h. At 0 h, there was a low density of small aggregates compared to that with Aβ incubated for 24 h, which showed a considerable amount of fibrillar growth consistent with our previous finding (*26*). Figure 1 illustrates the representative AFM images of Aβ co-incubated with different metal ions, grown over a solid template. The amount of fibrils formed was higher in the Fe^{3+}-induced Aβ aggregates (Figure 1) than in the Aβ incubated for 24 h in the absence of any metal (Figure S1). The co-incubation of Aβ with a single metal ion revealed amorphous, nonfibrillar morphology for Cu^{2+} and Zn^{2+} in contrast to the fibril formation with Fe^{3+}. Our results also showed that the final morphology of Aβ aggregates was not affected by the presence of metal-binding ligands or human serum albumin (Figure S2).

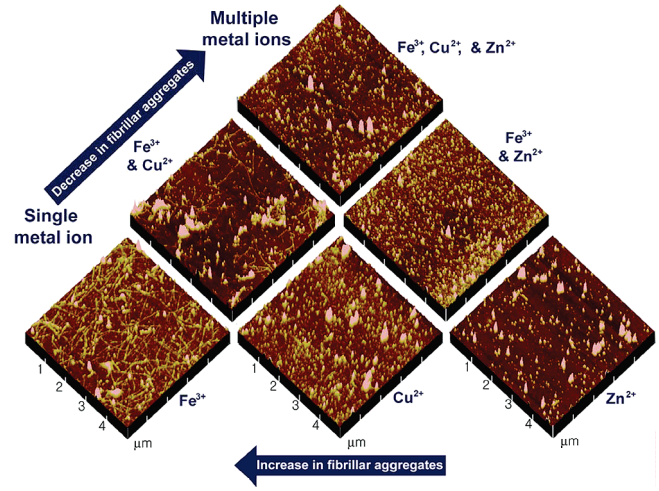

FIGURE 1: Representative AFM images of Aβ42 deposits formed over a solid surface by co-incubation of Aβ42 peptides: (from top to bottom right) with 100 μM Fe^{3+}, Cu^{2+}, and Zn^{2+}, with 100 μM Fe^{3+} and Cu^{2+}, with 100 μM Fe^{3+} and Zn^{2+}, with 100 μM Fe^{3+}, with 100 μM Cu^{2+}, or with 100 μM Zn^{2+}, respectively. The size of each AFM image is 5 μm × 5 μm.

When Aβ was co-incubated with Fe^{3+} and Cu^{2+} or Zn^{2+}, nonfibrillar, amorphous aggregates formed. The degree of deposition was also significantly reduced, as evidenced from the height versus frequency distribution plot of the multiple metal-induced Aβ aggregates (Figure S3). The Fe^{3+}-induced fibrillar aggregates had the distribution pattern corresponding to the greater heights of the aggregates, compared to those that were co-incubated with two or three metal ions (Figure S3). In the initial stage of Aβ aggregation from fresh monomers, we could observe the formation of small and spherical Aβ aggregates with a diameter of 10−15 nm. We further analyzed AFM images with PSD to investigate the effect of multiple metal ions on the initial stage of Aβ aggregation from fresh monomers (Figure S4). The PSD value for the sample co-incubated with Fe^{3+} alone was at least 10 times larger than those of other samples over the entire frequency domain, indicating that the initial rate of Aβ aggregation is also suppressed by the presence of Cu^{2+} or Zn^{2+}. These results highlighted the critical role of Cu^{2+}

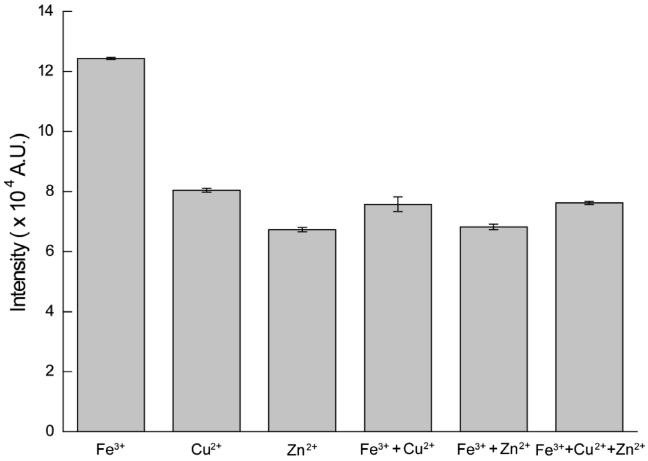

FIGURE 2: ThT fluorescence of Aβ42 plaques formed on solid templates in the presence of single or co-incubated multiple metal ions. The intensity of ThT fluorescence from each sample was subtracted from that of a bare glass.

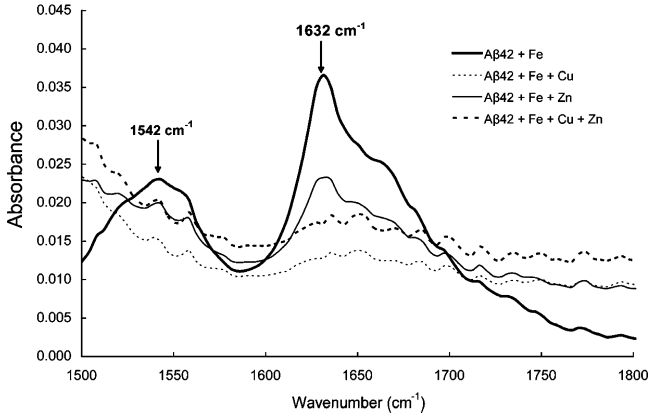

FIGURE 3: FTIR spectra of Aβ42 amyloid plaques induced by Fe^{3+} or mixed metal ions during co-incubation.

and Zn^{2+} in the decrease in the level of Aβ aggregation and also the degree of deposition when present with Fe^{3+}.

The induced fluorescence of ThT has been widely applied in studying amyloid formation because of its sensitivity and practicality (*29*). Figure 2 shows the ThT fluorescence induced by different types of Aβ deposits induced in the presence of one, two, or all three metal ions together. Results of a previous study indicated that Fe^{3+} induced fibrillar deposits, whereas Cu^{2+} or Zn^{2+} induced nonfibrillar amorphous aggregates of Aβ (*16, 26*). For the purposes of this study, we have utilized a template containing an Fe^{3+}-induced fibrillar deposit as a positive control for comparing the nature and extent of the deposits of other templates. Incubation with Fe^{3+} and Cu^{2+} induced an ~0.61-fold decrease, Fe^{3+} and Zn^{2+} an ~0.55-fold decrease, and Fe^{3+}, Cu^{2+}, and Zn^{2+} together an ~0.61-fold decrease in ThT fluorescence compared to Fe^{3+}-induced Aβ aggregation. It was also noted that, although Fe^{3+} alone enhanced Aβ fibrillation and Cu^{2+} or Zn^{2+} individually gave rise to nonfibrillar amorphous aggregates, the nature of aggregates became "nonfibrillar" when three ions were present together. The secondary structure of deposits formed on a solid template was analyzed by FTIR spectroscopy. Figure 3 shows the FTIR spectra of Aβ aggregates formed on the template in the absence or presence of Fe^{3+} only, or with Fe^{3+} and Cu^{2+} or Zn^{2+}, or with Fe^{3+}, Cu^{2+}, and Zn^{2+} together. Information about specific FTIR

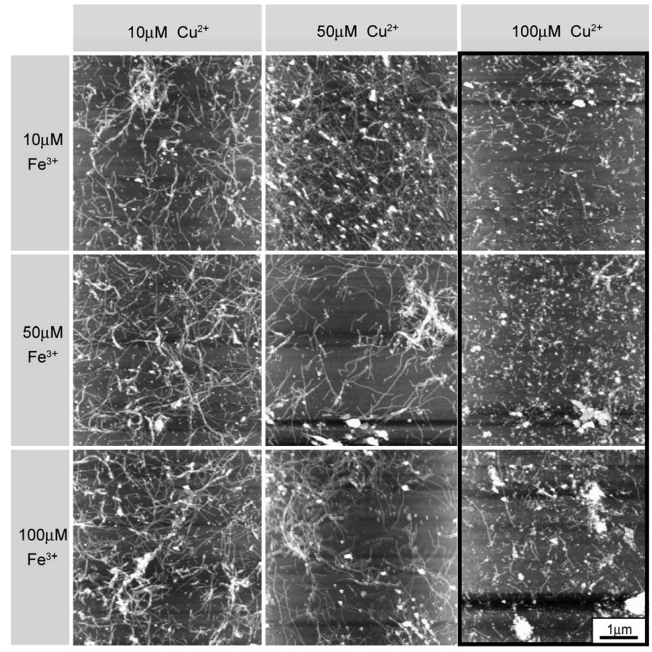

FIGURE 4: Effect of Cu^{2+} concentration (10, 50, and 100 μM) on the morphology of Aβ42 deposits formed in the presence of different concentrations of Fe^{3+} (10, 50, and 100 μM). The condition for sample preparation and the AFM analysis was the same as in Figure 1. The box outlines the AFM pictures representing dissociation of fibrillar aggregates by Cu^{2+} at 100 μM. The size of each AFM image is 5 μm × 5 μm, and the scale bar represents 1 μm.

peaks for the Aβ aggregates, formed in the presence of Fe^{3+}, indicated an amide I band with a relatively strong absorption peak at 1632 cm^{-1}, which depicted the presence of a dominant cross β-sheet structure in the amyloid aggregates. According to a previous study (*30*), an absorption spectrum in amide I and II bands was dependent on changes in the secondary structure of Aβ peptides. Aβ aggregates, in the absence of any metal ion, produced a spectrum with relatively reduced absorption peaks around 1632 cm^{-1}. The predominant amide I peaks at 1652 and 1670 cm^{-1} for Aβ deposits induced by Fe^{3+} and Cu^{2+} or by Fe^{3+}, Cu^{2+}, and Zn^{2+} indicated that Cu^{2+} and Zn^{2+} had a much higher binding affinity for Aβ and their presence yielded a predominant α-helix or random coil structure. Thus, one could speculate from the FTIR plots that, in the presence of only Fe^{3+}, Aβ displayed cross β-sheet structures whereas when co-incubated with multiple metal ions together yielded non-β-sheet structure, confirming that the co-incubation with multiple metal ions altered the conformation of the aggregated Aβ over a solid surface.

Dependence of Aβ Aggregation on the Concentrations of Multiple Metal Ions. To further explore the effect of Cu^{2+} or Zn^{2+}, which could control the possible alteration of the fibrillation process, we observed the concentration dependence of these ions over Fe^{3+} during Aβ aggregation. The co-incubation of different concentrations of Fe^{3+} with different amounts of either Cu^{2+} or Zn^{2+} was studied through ex situ AFM analysis. Consistent with the previous results of this study, the AFM images of Aβ grown with different concentrations of Fe^{3+} (10, 50, and 100 μM) and Cu^{2+} (10, 50, and 100 μM) indicated that some of the Fe^{3+}-induced Aβ fibrillar aggregates were still present when the Cu^{2+} concentration was low (10 or 50 μM), but the level of fibrils

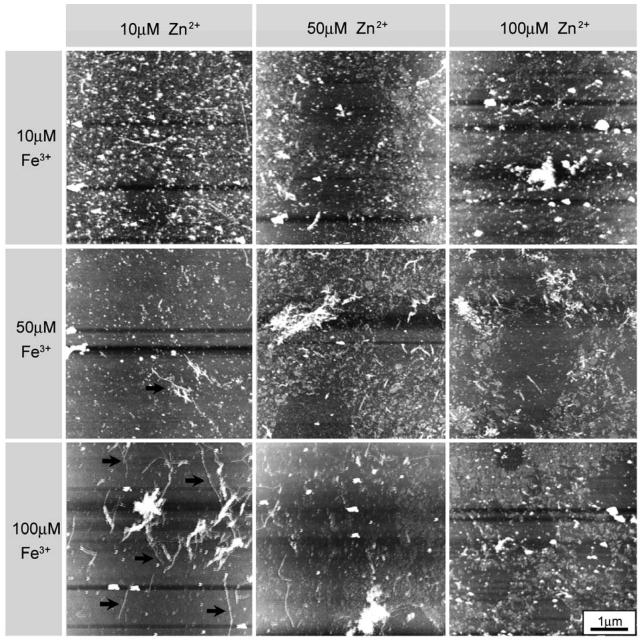

FIGURE 5: Effect of Zn^{2+} concentration (10, 50, and 100 μM) on the morphology of Aβ42 deposits formed in the presence of different concentrations of Fe^{3+} (10, 50, and 100 μM). Arrows point to amyloid fibrils longer than 500 nm. The condition for sample preparation and the AFM analysis was the same as in Figure 1. The size of each AFM image is 5 μm × 5 μm, and the scale bar represents 1 μm.

formed by Fe^{3+} was decreased at a higher concentration of Cu^{2+} (100 μM) (Figure 4). These findings indicate that high concentrations of Cu^{2+} were required for the formation of nonfibrillar, amorphous aggregates. In the previous results of this study, it was evident that, along with Cu^{2+}, Zn^{2+} was contributing to the alteration of fibrillar morphology. In this context, we further extended our investigation of the dependence of Aβ aggregation on Zn^{2+} concentration and its morphology. The Aβ deposition in combinations of Fe^{3+} and Zn^{2+} is shown in Figure 5. Freshly prepared Aβ (6 μM) peptide was co-incubated with different concentrations of Fe^{3+} (10, 50, and 100 μM) and Zn^{2+} (10, 50, and 100 μM). Although we observed several short fibrils (arrows) at higher concentrations of Fe^{3+} (50 and 100 μM), fibrillar morphology was not observed in the rest of the cases. The effect of Zn^{2+} clearly indicated that a lower concentration of Zn^{2+} than of Cu^{2+} was sufficient to change the Aβ fibrillation.

Sequential Addition of Cu^{2+} and Zn^{2+}. Once amyloid aggregates were formed on a solid surface, it also became important to investigate whether these aggregates could be affected by changing the metal ion dissolved in the solution phase. To observe the possible transition of Aβ aggregates from a fibrillar to a nonfibrillar, amorphous nature, we studied the sequential addition of metal ions, where the Fe^{3+}-induced Aβ fibrillar aggregates were further incubated "sequentially" with either Cu^{2+} or Zn^{2+}. The Aβ fibrillar assemblages formed by Fe^{3+} were found to be quite stable, as they retained a similar morphology when those fibrils were further incubated with a buffer-only solution (Figure 6). The representative AFM images in Figure 6 indicated that the sequential addition of Cu^{2+} or Zn^{2+} changed the nature of aggregates to nonfibrillar, amorphous forms. The AFM pictures supported the contention that, when the incubation solution was replaced with a lower concentration of Cu^{2+}, the fibrillar and amorphous nature both coexisted, suggesting that the low concentration was acting as a switch between these two forms. However, at the same concentration, Zn^{2+} could efficiently disintegrate the fibrils. Similar findings were also evidenced by using ThT fluorescence induction due to the different Aβ aggregates (Figure 7). Taking the amount of fluorescence of Fe^{3+}-induced fibrils to be unity, we found that the extent of fibril formation decreased ~0.65-fold for Cu^{2+} and decreased ~0.54-fold for Zn^{2+}. The decreased ThT fluorescence for the sequential addition of Cu^{2+} or Zn^{2+} indicated a sure reduction in the level of "amyloid" aggregates compared to Fe^{3+}-induced Aβ deposits.

DISCUSSION

According to the amyloid cascade hypothesis (*31*), the deposition of Aβ diffuse plaques is an initial step that may be associated with AD pathogenesis. Studies on the interaction of a single metal ion with Aβ and aggregation has been extensively explored (*20*−*22*), but it was more significant to investigate the involvement of multiple metal ions in Aβ aggregation and dissociation, as different metals reside in the brains of AD patients at high concentrations. We have designed a synthetic solid template by immobilizing Aβ oligomers onto a functionalized glass, and the deposition of a fresh Aβ over the template occurred in the presence of different combinations of either Cu^{2+}, Zn^{2+}, or Fe^{3+}. Results indicated that the presence of Cu^{2+} and Fe^{3+}, or Zn^{2+} and Fe^{3+}, decreased the amount of fibrillar amyloid deposition compared to that with Fe^{3+} alone (Figures 1 and S1). This observation indicates that Fe^{3+} might play an important role in fibrillar amyloid deposition, but the addition of Cu^{2+} or Zn^{2+} might have prevented the conformational change of Aβ to cross β-sheet structure, resulting in the reduction of fibrillar amyloid aggregates. The ThT fluorescence study also supported a similar finding, where a significant decrease in the fluorescence was observed when Aβ was incubated with Fe^{3+} and Cu^{2+}, Fe^{3+} and Zn^{2+}, or Fe^{3+}, Cu^{2+}, and Zn^{2+} (Figure 2). According to the analysis by FTIR spectroscopy (Figure 3), the Aβ aggregates formed in the presence of Fe^{3+} exhibited a dominant cross β-sheet structure, whereas in the presence of Cu^{2+} or Zn^{2+}, the Aβ aggregates yielded non-β-sheet structure. Our results suggest that Aβ aggregation and the decline in fibrillar morphology could be caused by the competition between metal ions for metal binding sites of Aβ peptides. Although it is well-established that Cu^{2+} and Zn^{2+} tend to bind the Aβ peptides with high affinity (*32*−*34*), the findings of this study indicate that the more efficient binding of Cu^{2+} or Zn^{2+} compared to Fe^{3+} may influence the stability of Aβ deposition and result in nonfibrillar amorphous forms.

To determine the Cu^{2+} concentration needed for reducing fibril formation, we analyzed via ex situ AFM the Aβ templates incubated with different concentrations of Fe^{3+} and Cu^{2+} (Figure 4). The results suggested that Cu^{2+} at a lower concentration did not affect the formation of fibrillar morphology and a concentration as high as 100 μM was required for the decrease in the level of fibrillation. It was previously reported that the copper binding site in aggregated Aβ changes with copper concentration (*35*−*37*). In addition, our previous study (*26*) suggested that the morphology of Aβ aggregates was fibrillar at a low concentration of Cu^{2+}

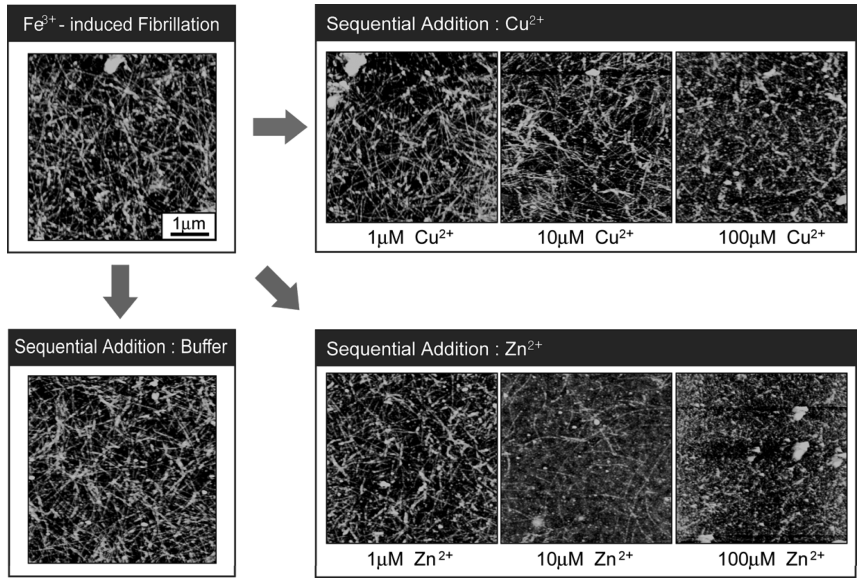

FIGURE 6: Effect of sequential addition of Fe^{3+}-induced fibrillar Aβ42 aggregates into either only buffer or buffer containing Cu^{2+} or Zn^{2+} at different concentrations (0, 1, 10, or 100 μM) on the morphology of deposits. The size of each AFM image is 5 μm × 5 μm, and the scale bar represents 1 μm.

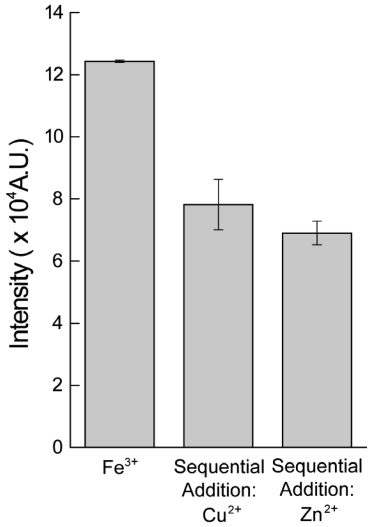

FIGURE 7: ThT fluorescence of Fe^{3+}-induced Aβ42 deposits with sequential addition of the template into a 100 μM solution of Cu^{2+} or Zn^{2+}. The conditions for the template preparation and the AFM analysis were the same as in Figure 6 except that only 100 μM metal ions were used. The intensity of ThT fluorescence from each sample was subtracted from that of a bare glass.

but became nonfibrillar amorphous at higher concentrations of Cu^{2+}. The findings of this study support this contention and extend it to suggest that Zn^{2+} was required at much lower concentrations to inhibit the Aβ aggregation compared to Cu^{2+}, when co-incubated together with Fe^{3+} (Figure 5). In vitro studies found that Zn^{2+}, at low micromolar concentrations, rapidly precipitated soluble Aβ into protease-resistant amyloid aggregates (*13*). This may be the reason why as little as 10 μM Zn^{2+} was sufficient to accelerate the formation of nonfibrillar deposits in this work. Taken together, our results suggest that the nature and amount of Aβ deposition could be affected by the interactions of varying concentrations of various metal ions.

Earlier studies demonstrated the effect of Cu^{2+} and Zn^{2+} on Aβ aggregation (*22, 35*), but little of the possible role of Cu^{2+} and Zn^{2+} in the dissociation of fibrillar amyloid plaques was explored. To further investigate the role of Cu^{2+} and Zn^{2+} in the dissociation of Aβ fibrils, we conducted the experiments with sequential addition of Cu^{2+} and Zn^{2+} to Fe^{3+}-induced Aβ aggregates. The Fe^{3+}-induced Aβ assemblages were incubated sequentially, in the absence of metal ion (i.e., buffer-only solution) or in the presence of either Cu^{2+} or Zn^{2+}. AFM images in Figure 6 suggest that Fe^{3+}-induced Aβ fibrillar assemblages were quite stable in a buffer solution. In contrast, Fe^{3+}-induced Aβ fibrils were conformationally changed by the sequential addition of Cu^{2+} or Zn^{2+}. In response to the gradual increase in the concentration, Zn^{2+} was found to dissociate most Aβ fibrils at a concentration of only 10 μM, and at a concentration of 100 μM, most fibrillar aggregates were dissociated to yield the amorphous form. The transition of Cu^{2+} between the two aggregate forms was centered close to 10 μM, where both forms of the peptide coexisted. However, at a higher concentration (100 μM), Cu^{2+} definitely dissociated the fibrillar aggregates induced by Fe^{3+}. This phenomenon implies that it is quite likely that Fe^{3+} is displaced from amyloid fibrils by Zn^{2+} or Cu^{2+}, which might contribute to the dissociation of Fe^{3+}-induced fibrillar aggregates. The degree of fibril dissociation was greatly reduced by the treatment with Zn^{2+}, compared to Cu^{2+}. Our findings with the sequential addition of metal ions on preformed Fe^{3+}-induced fibrils were further supported by a ThT fluorescence study (Figure 7). AFM and ThT fluorescence data together indicate that Aβ fibrillar aggregates induced by Fe^{3+} were conformationally changed to amorphous deposits when incubated further with Cu^{2+} or Zn^{2+}.

This work may be summarized as illustrated in Figure 8. The results from co-incubation experiments suggest that, when Fe^{3+}-induced Aβ assemblages are co-incubated with a fresh Aβ solution containing Cu^{2+} and/or Zn^{2+} with Fe^{3+}, the morphology of aggregates becomes nonfibrillar. Data from ex situ AFM studies and ThT fluorescence data of fibrillar templates with sequential addition of Cu^{2+} or Zn^{2+} point to the importance of metal ions in fibril dissociation. It is likely that the metal ions are present in suprastoichio-

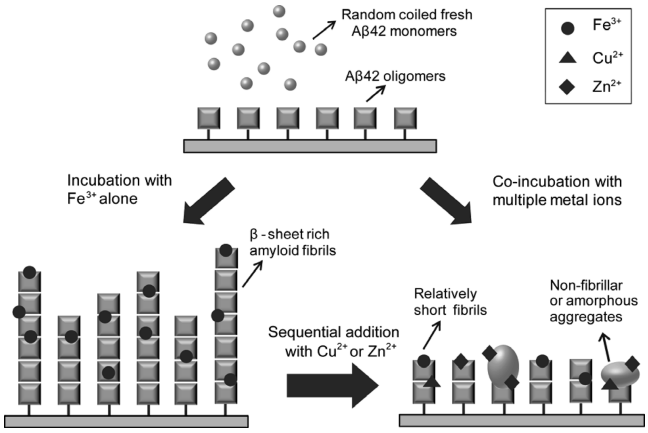

FIGURE 8: Proposed hypothesis for the Aβ aggregation due to co-incubation of Fe^{3+}, Zn^{2+}, and Cu^{2+} and sequential addition of Cu^{2+} and/or Zn^{2+} to Fe^{3+}-induced Aβ fibrillar aggregates.

metric ratios with respect to Aβ in the diseased brain of AD patients, which generates the possibility of the presence of both fibrillar and amorphous aggregates of Aβ together, thereby making our study more relevant. Furthermore, the decrease in the level of fibrillation and the increase in the number of amorphous deposits could be protective to cells as Huang et al. (*38*) showed earlier that the amorphous form of Aβ was not associated with neurodegeneration. Further studies involving the cellular toxicity due to the different forms of Aβ aggregates induced by metal ion(s) are currently under progress. Figure S5 shows our preliminary result about the cell viability over Aβ templates prepared in the presence of different metal ions. When cells were cultured on the Aβ templates prepared with Fe^{3+}, Cu^{2+}, and Zn^{2+}, cell viability was reduced to 50, 55, and 71%, respectively. Our results are consistent with previous studies (*27, 39*), which reported that the neurotoxicity of Aβ is mediated by iron or copper that is redox-active and produces hydrogen peroxide, but zinc reduces the Aβ toxicity.

In conclusion, the results of this study indicate that the balance of metal ions such as Cu^{2+}, Zn^{2+}, and Fe^{3+} might play an important role in determining the morphology of Aβ aggregation or its dissociation. These results and our interpretation may provide an insight into the role of interactions of multiple metal ion with Alzheimer's Aβ or its aggregates.

SUPPORTING INFORMATION AVAILABLE

Additional data showing AFM images for the oligomerization and fibrillation of Aβ in the presence of multiple metal ions and the cell viability over Aβ templates prepared in the presence of different metal ions. This material is available free of charge via the Internet at http://pubs.acs.org.

REFERENCES

1. Knowles, R. B., Wyart, C., Buldyrev, S. V., Cruz, L., Urbanc, B., Hasselmo, M. E., Stanley, H. E., and Hyman, B. T. (1999) Plaque-induced neurite abnormalities: Implications for disruption of neural networks in Alzheimer's disease. *Proc. Natl. Acad. Sci. U.S.A. 96*, 5274–5279.
2. Tanzi, R. E., Gusella, J. F., Watkins, P. C., Bruns, G. A., St. George-Hyslop, P., Van Keuren, M. L., Patterson, D., Pagan, S., Kurnit, D. M., and Neve, R. L. (1987) Amyloid β protein gene: cDNA, mRNA distribution, and genetic linkage near the Alzheimer locus. *Science 235*, 880–884.
3. Kang, J., Lemaire, H. G., Unterbeck, A., Salbaum, J. M., Masters, C. L., Grzeschik, K. H., Multhaup, G., Beyreuther, K., and Muller-Hill, B. (1987) The precursor of Alzheimer's disease amyloid A4 protein resembles a cell-surface receptor. *Nature 325*, 733–736.
4. Lambert, M. P., Barlow, A. K., Chromy, B. A., Edwards, C., Freed, R., Liosatos, M., Morgan, T. E., Rozovsky, I., Trommer, B., Viola, K. L., Wals, P., Zhang, C., Finch, C. E., Krafft, G. A., and Klein, W. L. (1998) Diffusible, nonfibrillar ligands derived from Aβ1−42 are potent central nervous system neurotoxins. *Proc. Natl. Acad. Sci. U.S.A. 95*, 6448–6453.
5. Dahlgren, K. N., Manelli, A. M., Stine, W. B., Baker, L. K., Krafft, G. A., and LaDu, M. J. (2002) Oligomeric and fibrillar species of amyloid-β peptides differentially affect neuronal viability. *J. Biol. Chem. 277*, 32046–32053.
6. Chromy, B. A., Nowak, R. J., Lambert, M. P., Viola, K. L., Chang, L., Velasco, P. T., Jones, B. W., Fernandez, S. J., Lacor, P. N., Horowitz, P., Finch, C. E., Krafft, G. A., and Klein, W. L. (2003) Self-Assembly of Aβ1−42 into globular neurotoxins. *Biochemistry 42*, 12749–12760.
7. Lorenzo, A., and Yankner, B. A. (1994) β-Amyloid neurotoxicity requires fibril formation and is inhibited by congo red. *Proc. Natl. Acad. Sci. U.S.A. 91*, 12243–12247.
8. Weldon, D. T., Rogers, S. D., Ghilardi, J. R., Finke, M. P., Cleary, J. P., O'Hare, E., Esler, W. P., Maggio, J. E., and Mantyh, P. W. (1998) Fibrillar β-amyloid induces microglial phagocytosis, expression of inducible nitric oxide synthase, and loss of a select population of neurons in the rat CNS in vivo. *J. Neurosci. 18*, 2161–2173.
9. Moir, R. D., Atwood, C. S., Romano, D. M., Laurans, M. H., Huang, X., Bush, A. I., Smith, J. D., and Tanzi, R. E. (1999) Differential effects of apolipoprotein E isoforms on metal-induced aggregation of Aβ using physiological concentrations. *Biochemistry 38*, 4595–4603.
10. Bush, A. I. (2003) The metallobiology of Alzheimer's disease. *Trends Neurosci. 26*, 207–214.
11. Selkoe, D. J. (2001) Alzheimer's disease: Genes, proteins, and therapy. *Physiol. Rev. 81*, 741–766.
12. Lovell, M. A., Robertson, J. D., Teesdale, W. J., Campbell, J. L., and Markesbery, W. R. (1998) Copper, iron and zinc in Alzheimer's disease senile plaques. *J. Neurol. Sci. 158*, 47–52.
13. Bush, A. I., Pettingell, W. H., Multhaup, G., de Paradis, M., Vonsattel, J. P., Gusella, J. F., Beyreuther, K., Masters, C. L., and Tanzi, R. E. (1994) Rapid induction of Alzheimer Aβ amyloid formation by zinc. *Science 265*, 1464–1467.
14. Burkoth, T. S., Benzinger, T. L. S., Urban, V., Morgan, D. M., Gregory, D. M., Thiyagarajan, P., Botto, R. E., Meredith, S. C., and Lynn, D. G. (2000) Structure of the β-amyloid(10−35) fibril. *J. Am. Chem. Soc. 122*, 7883–7889.
15. Bush, A. I., and Tanzi, R. E. (2002) The galvanization of β-amyloid in Alzheimer's disease. *Proc. Natl. Acad. Sci. U.S.A. 99*, 7317–7319.
16. Zou, J., Kajita, K., and Sugimoto, N. (2001) Cu^{2+} inhibits the aggregation of amyloid β-peptide (1−42) in vitro. *Angew. Chem., Int. Ed. 40*, 2274–2277.
17. Morgan, D. M., Dong, J., Jacob, J., Lu, K., Apkarian, R. P., Thiyagarajan, P., and Lynn, D. G. (2002) Metal switch for amyloid formation: Insight into the structure of the nucleus. *J. Am. Chem. Soc. 124*, 12644–12645.
18. Arispe, N., Pollard, H. B., and Rojas, E. (1996) Zn^{2+} interaction with Alzheimer amyloid β protein calcium channels. *Proc. Natl. Acad. Sci. U.S.A. 93*, 1710–1715.
19. Curtain, C. C., Ali, F., Volitakis, I., Cherny, R. A., Norton, R. S., Beyreuther, K., Barrow, C. J., Masters, C. L., Bush, A. I., and Barnham, K. J. (2001) Alzheimer's disease amyloid-β binds copper and zinc to generate an allosterically ordered membrane-penetrating structure containing superoxide dismutase-like subunits. *J. Biol. Chem. 276*, 20466–20473.
20. Exley, C. (2006) Aluminium and iron, but neither copper nor zinc, are key to the precipitation of β-sheets of Aβ42 in senile plaque cores in Alzheimer's disease. *J. Alzheimer's Dis. 10*, 173–177.
21. House, E., Collingwood, J., Khan, A., Korchazkina, O., Berthon, G., and Exley, C. (2004) Aluminium, iron, zinc and copper influence the in vitro formation of amyloid fibrils of Aβ42 in a manner which may have consequences for metal chelation therapy in Alzheimer's disease. *J. Alzheimer's Dis. 6*, 291–301.
22. Garai, K., Sengupta, P., Sahoo, B., and Maiti, S. (2006) Selective destabilization of soluble amyloid β oligomers by divalent metal ions. *Biochem. Biophys. Res. Commun. 345*, 210–215.

23. Esler, W. P., Stimson, E. R., Jennings, J. M., Ghilardi, J. R., Mantyh, P. W., and Maggio, J. E. (1996) Zinc-induced aggregation of human and rat β-amyloid peptides in vitro. *J. Neurochem. 66*, 723–732.
24. Atwood, C. S., Moir, R. D., Huang, X., Scarpa, R. C., Bacarra, N. M. E., Romano, D. M., Hartshorn, M. A., Tanzi, R. E., and Bush, A. I. (1998) Dramatic aggregation of Alzheimer Aβ by Cu(II) is induced by conditions representing physiological acidosis. *J. Biol. Chem. 273*, 12817–12826.
25. Ha, C., and Park, C. B. (2006) *Ex situ* atomic force microscopy analysis of β-amyloid self-assembly and deposition on a synthetic template. *Langmuir 22*, 6977–6985.
26. Ha, C., Ryu, J., and Park, C. B. (2007) Metal ions differentially influence the aggregation and deposition of Alzheimer's β-amyloid on a solid template. *Biochemistry 46*, 6118–6125.
27. Huang, X., Atwood, C. S., Hartshorn, M. A., Multhaup, G., Goldstein, L. E., Scarpa, R. C., Cuajungco, M. P., Gray, D. N., Lim, J., Moir, R. D., Tanzi, R. E., and Bush, A. I. (1999) The Aβ peptide of Alzheimer's disease directly produces hydrogen peroxide through metal ion reduction. *Biochemistry 38*, 7609–7616.
28. Libertino, S., Giannazzo, F., Aiello, V., Scandurra, A., Sinatra, F., Renis, M., and Fichera, M. (2008) XPS and AFM characterization of the enzyme glucose oxidase immobilized on SiO_2 surfaces. *Langmuir 24*, 1965–1972.
29. LeVine, H. (1993) Thioflavine T interaction with synthetic Alzheimer's disease β-amyloid peptides: Detection of amyloid aggregation in solution. *Protein Sci. 2*, 404–410.
30. Lin, S.-Y., and Chu, H.-L. (2003) Fourier transform infrared spectroscopy used to evidence the prevention of β-sheet formation of amyloid β (1−40) peptide by a short amyloid fragment. *Int. J. Biol. Macromol. 32*, 173–177.
31. Hardy, J., and Selkoe, D. J. (2002) The amyloid hypothesis of Alzheimer's disease: Progress and problems on the road to therapeutics. *Science 297*, 353–356.
32. Atwood, C. S., Scarpa, R. C., Huang, X., Moir, R. D., Jones, W. D., Fairlie, D. P., Tanzi, R. E., and Bush, A. I. (2000) Characterization of copper interactions with Alzheimer amyloid β peptides: Identification of an attomolar-affinity copper binding site on amyloid β1−42. *J. Neurochem. 75*, 1219–1233.
33. Dong, J., Atwood, C. S., Anderson, V. E., Siedlak, S. L., Smith, M. A., Perry, G., and Carey, P. R. (2003) Metal binding and oxidation of amyloid-β within isolated senile plaque cores: Raman microscopic evidence. *Biochemistry 42*, 2768–2773.
34. Syme, C. D., Nadal, R. C., Rigby, S. E. J., and Viles, J. H. (2004) Copper binding to the amyloid-β (Aβ) peptide associated with Alzheimer's disease. *J. Biol. Chem. 279*, 18169–18177.
35. Smith, D. P., Ciccotosto, G. D., Tew, D. J., Fodero-Tavoletti, M. T., Johanssen, T., Masters, C., Barnham, K. J., and Cappai, R. (2007) Concentration dependent Cu^{2+} induced aggregation and dityrosine formation of the Alzheimer's disease amyloid-β peptide. *Biochemistry 46*, 2881–2891.
36. Jun, S., and Saxena, S. (2007) The aggregated state of amyloid-β peptide in vitro depends on Cu^{2+} ion concentration. *Angew. Chem., Int. Ed. 46*, 1–4.
37. Dong, J., Shokes, J. E., Scott, R. A., and Lynn, D. G. (2006) Modulating amyloid self-assembly and fibril morphology with Zn(II). *J. Am. Chem. Soc. 128*, 3540–3542.
38. Huang, T. H. J., Yang, D.-S., Fraser, P. E., and Chakrabartty, A. (2000) Alternate aggregation pathways of the Alzheimer β-amyloid peptide. *J. Biol. Chem. 275*, 36436–36440.
39. Cuajungco, M. P., Goldstein, L. E., Nunomura, A., Smith, M. A., Lim, J. T., Atwood, C. S., Huang, X., Farrag, Y. W., Perry, G., and Bush, A. I. (2000) Evidence that the β-amyloid plaques of Alzheimer's disease represent the redox-silencing and entombment of Aβ by zinc. *J. Biol. Chem. 26*, 19439–19442.

BI800012E